





Scour Downstream of a Corrugated Apron under Free Jets

Rakesh Kumar Chaudhary¹ 
 Mohammad Aamir^{2*} 
 Zulfeqar Ahmad² 
 Surendra Kumar Mishra¹ 



¹Department of Water Resources Development and Management, Indian Institute of Technology Roorkee, India

²Department of Civil Engineering, Indian Institute of Technology Roorkee, India

*Corresponding author email: mohdaamir.amu@gmail.com

Received:
Sept. 08, 2019
Accepted:
Sept. 15, 2019
Published online:
Sept. 16, 2019

Abstract: The performance of corrugated apron under free flow subcritical condition over the apron was evaluated experimentally. Compared to smooth rigid apron, the scour depth increased with application of corrugated apron under free flow of jets. Velocity and turbulence characteristics as well as Reynolds shear stress over smooth and corrugated aprons were also studied. Rate of increase of turbulence intensity in scour hole due to smooth apron was found to be higher than scour hole due to corrugated apron. Scour downstream of corrugated apron clearly shows three distinct regions: jet diffusion, transition and accelerating region as well as recirculating region at near bed of scour hole.

Keywords: Corrugated apron, Froude number, Scour, Wall jets, Free surface flow

1. Introduction

Generally, virgin flow of channel gets disturbed by constructing hydraulic structures across it. By placing any structure across a channel, the natural flow gets modified near vicinity of structures. Flow either gets accelerated or decelerated, i.e. depth and velocity of flow does not remain same as in natural state before placing any structures across it. This leads to either aggradation or degradation of natural bed level. When flow approaches hydraulic structures, it gets decelerated and when it leaves such structures, it gets accelerated and tries to impose extra momentum acquired during accelerating stage to mobile bed surface. Once shear stress possessed by flowing water exceeds tractive shear stress of sediment, particle starts to move along flow direction. When shear stress possessed by flowing fluid exceeds critical shear stress of sediment, it starts to move. It leads to formation of local scour hole. Hydraulic structures mostly built across channels have to be protected against erosion occurring in their vicinity, specifically those founded on loose soils, also known as local scour. To determine the type of protection works required, it is essential to study the scour profile, its dimensions and flow characteristics within scour hole [1-13]. Several types of appurtenances such as chutes, sills and baffle blocks are often installed in stilling basin for flow stabilization by creating higher turbulence for dissipating energy. Hydraulic jump type stilling basins for low to high Froude numbers have been proposed by Peterka [14]. In his experimental study,

Helal et al. [15] used sills of different heights and positions for reducing scour. It was found that the higher sill and fully covered floor yielded less scour, and vice versa. Similarly, Pillai and Unny [16] studied the effects of different shapes of baffle blocks and found that the wedge-shaped blocks with vertex angle of 120° dissipated more energy in shorter length than rectangular blocks. Helal et al. [15] found that the use of floor water jets reduced scour depth by 50% to 90% and scour hole length by 42% to 85% compared to the floor without water jets. According to Dey and Sarkar [7], a launching apron of stones placed downstream of solid apron on mobile bed of length 2ds and stone size 18 mm (as per IRC89) can reduce scour depth ranging from 57.3% to 16.2% with average of 39%. Aamir and Ahmad [17] have put forward a comprehensive review on scour under wall jets.

Rajaratnam and Ead [18] pioneered the study of flow characteristics of submerged jump on corrugated apron. Ali et al. [19] used different sets of triangular strips of corrugated apron with spaced corrugations. The scour depth and length was reduced for fine sand by 63.4% and 30.2% respectively, and for coarse sand, by 44.2% and 20.6% respectively, with respect to that occurring in classical jump. It was also found that minimum scour depth occurred at optimal spacing ratio $s/t = 3$, as well as scour depth and length varies inversely with mean diameter of grain size particle. Basiouny et al. [20] used

U-shaped corrugated apron and found that average scour depth and length reduces by 44% and 29% respectively in comparison with smooth apron.

Most of the study regarding scour minimization have been done on submerged flow condition since dissipation of energy is achieved in hydraulic jump. Sometimes it becomes necessary to fully open sluice gate of canal regulators during maintenance, flushing sediment and when water level in parent canal is very low, and flow becomes free flow jet. In this condition scour hole dimension, which gets formed downstream of corrugated apron may differ from the submerged jump flow condition and it becomes essential for study. Triangular corrugated apron is not pragmatic as the triangular pointed crest changes to sinusoidal corrugation with time due to abrasion. Besides this, no study of variation in turbulence structures in scour hole due to corrugated apron have been performed. Therefore, the main objective of this paper is to study the variation in scour hole dimension and turbulence characteristics of scour hole.

2. Materials and Method

2.1 Experimental setup

The experiments were conducted in the Hydraulics laboratory of the Department of Civil Engineering, Indian Institute of Technology Roorkee, India. The flume was 10 m in length, 0.60 m wide and 0.54 m in depth. It consisted of electrically operated tail and sluice gates provided with adjustable rack and pinion arrangement to adjust depth of flow. The inlet discharge was adjusted with the valve fitted to the inlet pipe. Under the sluice gate, a concrete apron of size 1.0 m (top), 1.3 m (bottom), 0.6 m wide and 0.2 m deep was casted as shown in Figure 1. On smooth concrete apron floor, a smooth acrylic sheet (for smooth apron) of size 0.6 m \times 0.6 m was placed and fixed with concrete apron so that it does not float. The channel bed of 1.9 m length and 0.6 m width had 0.2 m depth of uniform sand of median size $d_{50} = 1.8$ mm.

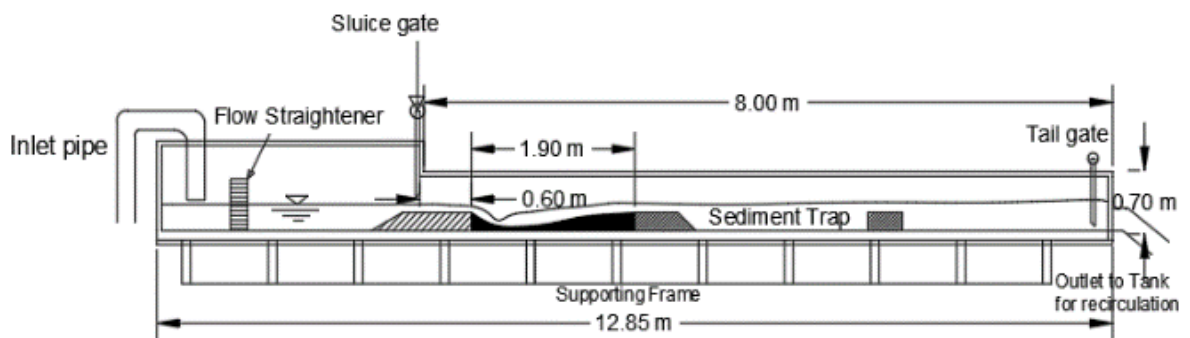


Fig 1 Elevation view of experimental flume for runs in free wall jet condition

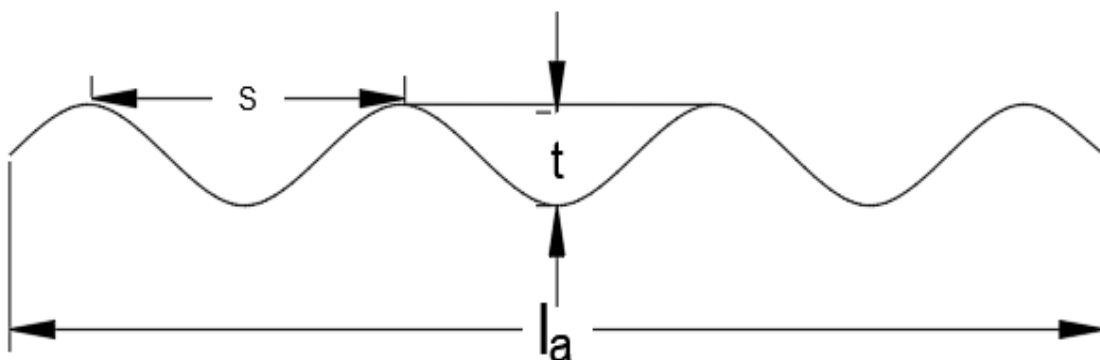


Fig 2 Definition sketch of corrugations

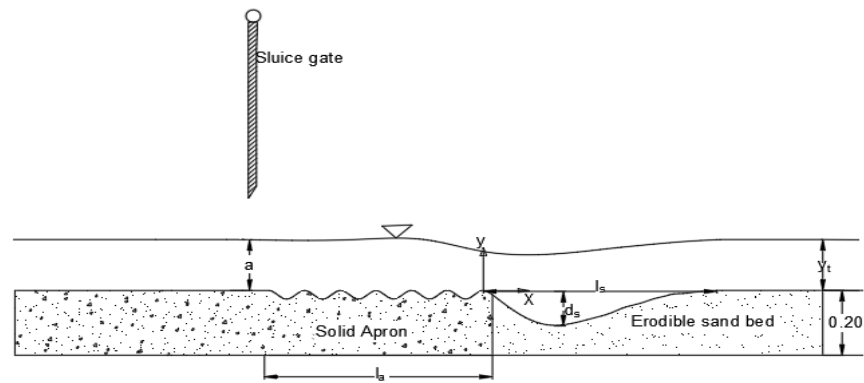


Fig 3 Definition sketch of scour downstream of corrugated apron in subcritical free flow condition

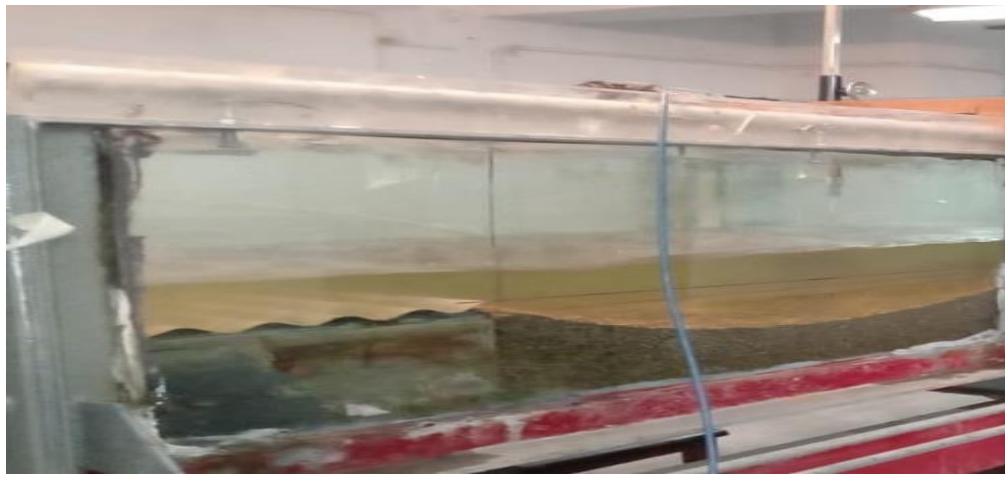


Fig 4 Photometric view of scour profile in free flow condition

Corrugated aprons used in experiments were made of GI sheet having set of (wave length s , amplitude t) as (65 mm, 15 mm), (70 mm, 15 mm), (70 mm, 20 mm) and (70 mm, 25 mm). Figure 2 shows the definition sketch of corrugation used in the experiments. The properties of sand were: median size $d_{50} = 1.8$ mm, geometric standard deviation $\sigma_g = 1.15$, sorting coefficient $S_o = 1.06$, coefficient of uniformity $C_u = 1.37$, specific gravity of sediment $G = 2.65$ and angle of repose $\phi = 31.5^\circ$.

2.2 Experimental procedure

In free flow subcritical condition, discharge was kept constant and only tailwater depth was varied. Sluice gate was fully opened with no pressurized flow so that the incoming flow remained subcritical (Figure 3). Four different tailwater depths were considered. For each tailwater depth, scour profiles were measured. Scour profiles were traced on tracing paper attached with flume glass (Figure 4). This procedure was done for both smooth and corrugated aprons. Maximum scour bed obtained was dried and then it was uniformly sprayed with synthetic resin mixed with water to make the scour bed rigid. Flow data were measured using Nortek Vectrino 5 cm down looking ADV having four probes. Sampling frequency was adjusted to 50 Hz and sampling time was 3-5 min. Flow and turbulence characteristics remained unaffected due to stabilization of scour hole.

Initially, sand bed was covered with ply board and pressed with some weights over ply board to prevent its movement. Discharge was fixed and only sluice gate opening was varied for each run. When desired tailwater gets achieved and flow becomes steady, then ply board cover was removed slowly so that it does not create any disturbance on sand bed. Temporal variation of scour profile was drawn on tracing paper as scour proceeds. Time interval for temporal variation was 2, 5, 15, 30, 45, 60, 120, and 360 minutes. The scour profile was two dimensional. Smooth rigid apron acts as bench mark for comparison of scour using corrugated apron under same flow condition as in smooth apron.

Measurement of scour profiles and hydraulic parameters were carried out for at least four sets of upstream gate openings, for each corrugated apron model. Discharge measurement was carried out with ultrasonic flow meter. Flow depth was measured with pointer gauge having accuracy of 0.1 mm.

3. Results and Discussion

The primary aim of experiments was to study scour downstream of corrugated aprons under free jet condition and to study turbulence in scour hole. Effect of various parameters on scour depth and length were analyzed graphically. Dimensional analysis was carried

out to establish the most affecting parameters for maximum scour depth and length.

3.1. Dimensional analysis

The maximum scour depth (*d*) and scour length (*l*) downstream of a corrugated apron can be expressed as a function of the following independent variables:

$$d_s, l_s = f(g, \rho, \rho_s, \mu, a, y_t, v_1, S, t, d_{50}, l_a) \quad (1)$$

where *g* is acceleration due to gravity, ρ is density of flowing water, ρ_s is density of sand, σ is geometric standard deviation of sediment particles, μ is viscosity of water, *a* is incoming flow depth (sluice gate opening), *y_t* is tailwater depth of jump, *v₁* is incoming flow velocity, *S* is the corrugation wavelength, *t* is its amplitude, *d₅₀* is median size of sediment, *l_a* is length of apron.

Taking ρ, v_1, a as repeating variables and using Buckingham Π theorem, following is obtained:

$$\frac{d_s}{a} = f\left(\frac{v_1}{\sqrt{ga}}, \frac{\rho_s}{\rho}, \frac{\rho a v_1}{\mu}, \frac{y_t}{a}, \frac{s}{a}, \frac{t}{a}, \frac{d_{50}}{a}, \frac{l_a}{a}\right) \quad (2)$$

$$\frac{l_s}{a} = f\left(\frac{v_1}{\sqrt{ga}}, \frac{\rho_s}{\rho}, \frac{\rho a v_1}{\mu}, \frac{y_t}{a}, \frac{s}{a}, \frac{t}{a}, \frac{d_{50}}{a}, \frac{l_a}{a}\right) \quad (3)$$

3.2. Scour under free flow condition

Free flow subcritical also known as modular flow exists downstream of sluice gate when either sluice gate is fully opened or both sluice gate and tail gate are open, i.e.

flow is not restricted by gate. In this study, only sluice gate was opened fully so that flow does not get restricted. Tail gate was operated to vary tailwater depth.

3.2.1. Scour profiles

Scouring of bed occurs when shear stress exerted by flowing jet of water exceeds threshold bed shear stress of sediment particles. As the run starts under particular free flow condition, scouring process starts which varies with time up to equilibrium scour profile. Initially, shear stress exerted at near bed by jet was high so rate of scour was also high. As the scour depth goes on increasing, shear stress at near bed exerted by jet goes on decreasing. In free flow jet, there is no formation of dune. It is due to the fact that there is no reversal of flow as well as no submergence. The shear stress possessed by the flowing jet at near bed was higher than submerged jump condition and due to this, bed material does not get mounded. The scoured sediment gets transported continuously from scour hole and moves towards downstream (Figures 5 and 6). Initially scour dimension increases at very fast rate later on it decrease with time. Rate of increase of horizontal dimension is larger than vertical dimension. Figure 6 shows scour profile obtained due to corrugated apron. In this scour depth increases and maximum depth shifts towards upstream in comparison with smooth rigid apron. It differs from Figure 5 which is the scour profile due to smooth rigid apron.

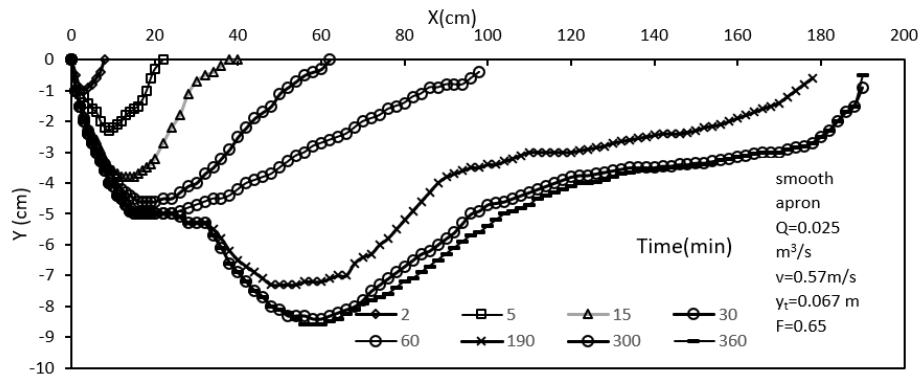


Fig 5 Development of scour profile with time up to asymptotic state for smooth apron.

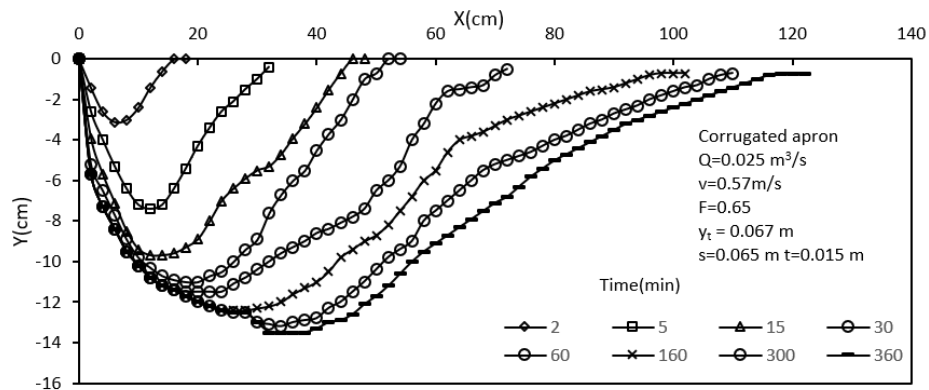


Fig 6 Development of scour profile with time up to asymptotic state for corrugated apron.

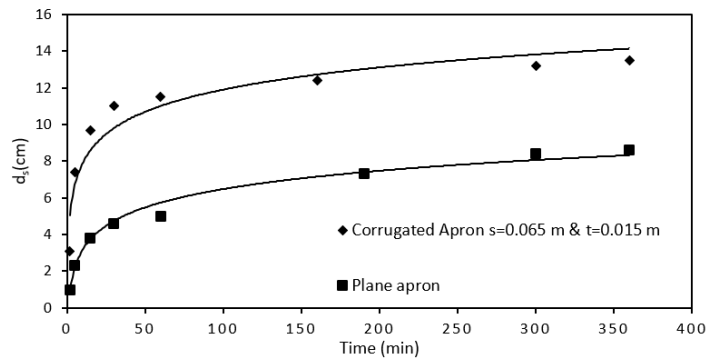


Fig 7 Temporal variation of scour for smooth and corrugated aprons under same flow condition.

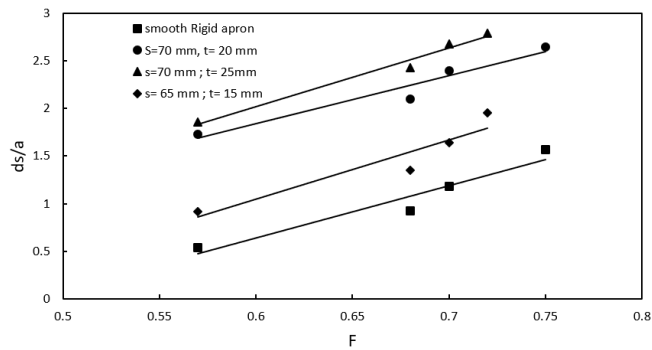


Fig 8 Variation of normalized scour depth with Froude number

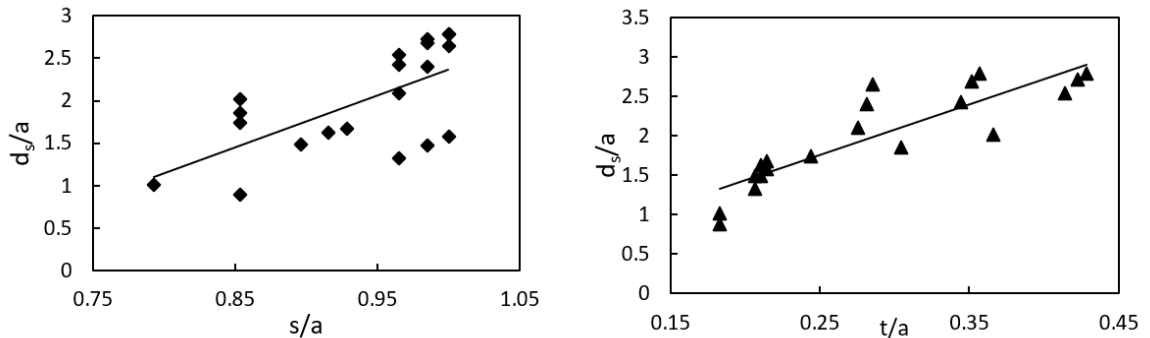


Fig 9 Variation of normalized maximum scour depth with (a) s/t and (b) t/a

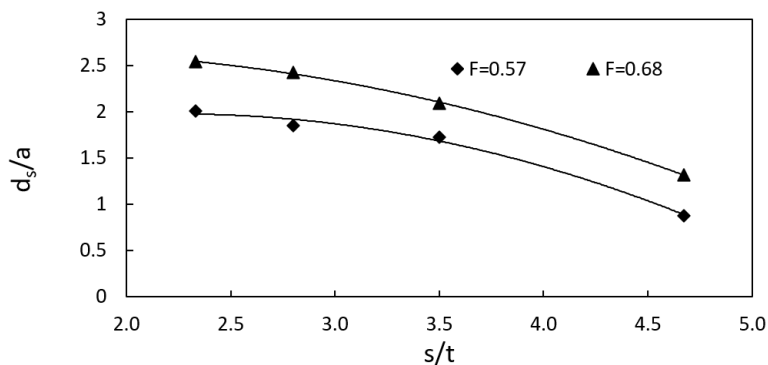


Fig 10 Variation of normalized maximum scour depth with s/t ratio

As seen from Figure 7, temporal variation of scour depth for smooth and corrugated apron shows that initially rate of scour is high up to substantial time, and later it decreases with time.

3.2.2. Effect of various parameters on maximum scour depth

(a) Effect of Froude number

Variation of scour depth was studied with incoming free jet Froude number $F = V/\sqrt{g^*a}$, where a is the flow depth just upstream of apron and V is the average approach velocity of jet just upstream of apron. When normalized with a , the scour depth varied linearly with Froude number as shown in Figure 8. Similarly, the results of Figures 5 - 7 show that, in free flow condition, the scour due to corrugated apron is larger than that due to smooth apron.

(b) Effect of s/a and t/a

Normalized maximum scour depth was plotted with normalized wavelength s/a and amplitude t/a , as shown in Figure 9. As s/a and t/a increases scour depth also increases and vice versa.

(c) Effect of spacing ratio s/t

Figure 10 clearly illustrates that as the normalized scour depth initially decreases at very slow rate with slight increase in s/t ratio. Further increase in s/t ratio will cause increase in normalized scour depth rapidly. It is obtained for range of s/t from 2.3 to 4.67.

(d) Effect of tailwater depth

As shown in Figure 11, it was found that as tailwater depth y_t increases, scour depth d_s decreases and at certain limiting tailwater depth, further increase in tailwater depth causes no increase in scour depth.

3.2.3 Distribution of velocity vector

Velocity vector plot over the apron and within scour hole is shown in Figures 12 and 13 for smooth and corrugated apron. Magnitude of velocity vector $U = \sqrt{u^2 + v^2}$, and direction of vector, $\theta = \tan^{-1} \frac{v}{u}$. Velocity over apron is found to increase more rapidly than within scour hole, which shows that growth rate of boundary layer in smooth apron is less than scour hole. This was same in both smooth and corrugated aprons. In case of corrugated apron which resulted in larger scour hole, growth rate of boundary layer was higher than smooth apron since velocity decreases with increase in scour depth. Scour hole formed downstream of smooth rigid apron is small in size compared to corrugated apron on same flow condition as shown in figure 12. Vector plots at the edge of smooth apron and just 0.1 m downstream of apron edge in scour hole clearly indicates that there is slight change in velocity vector at near bed of scour hole

which is due to change in roughness of surface. It follows logarithmic curve law. As we move from one section to next section downstream, the diffused free jet again slowly reunites and accelerates towards downstream. There is no any recirculation zone at the bed of scour hole, it only occurs in deep scour hole.

Similarly, in scour hole downstream of corrugated apron at near bed there is recirculation zone as scour hole is deep. As flow leaves apron and enters in scour hole it gets diffused and after that flow passes through transition region in which there is no much change in velocity vector and its magnitude. Then after it leaves scour hole and starts accelerating as flow depth also decreases which helps in gaining the lost velocity. It is clearly shown in Figure 13.

3.2.4 Distribution of turbulence intensity

Vertical distribution of normalized turbulence intensity for both smooth and corrugated aprons was plotted as shown in Figure 15. Horizontal normalized turbulence intensity $TI_x = (\overline{u'u'})^{0.5} / V$, where u' = fluctuation of u from mean velocity at that point along X direction = $u - \bar{u}$ and V = average approach flow velocity of free flow jet, i.e. mean velocity of flow at sluice gate. Similarly, vertical normalized turbulence intensity $TI_y = (\overline{v'v'})^{0.5} / V$; v' = fluctuation of v from mean along Y direction = $v - \bar{v}$. Horizontal normalized turbulence intensity TI_x increases gradually from bottom of apron at (0,0) for a short distance along Y axis and then reduces slightly and finally attains constant value. This trend is same in both smooth and corrugated aprons. It is the major cause of larger scour dimension for corrugated apron than smooth apron. Similarly, TI_x at near bed is higher in case of scour downstream of smooth apron than scour due to corrugated apron. It reduces in upper layers for smooth apron showing less turbulence near surface. In case of corrugated apron TI_x near scoured bed is low and goes on increasing along vertical Y direction. Overall, the magnitude of turbulence intensity is higher for corrugated apron than smooth apron at every section of measurement, as shown in Figure 14.

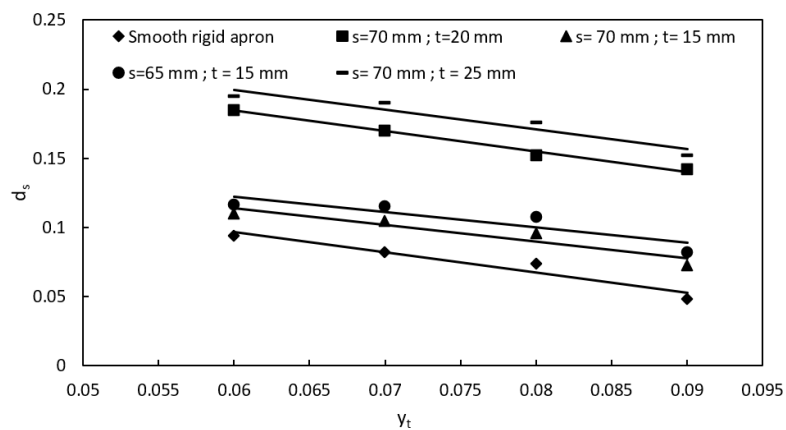


Fig 11 Variation of maximum scour depth d_s with tail water depth y_t

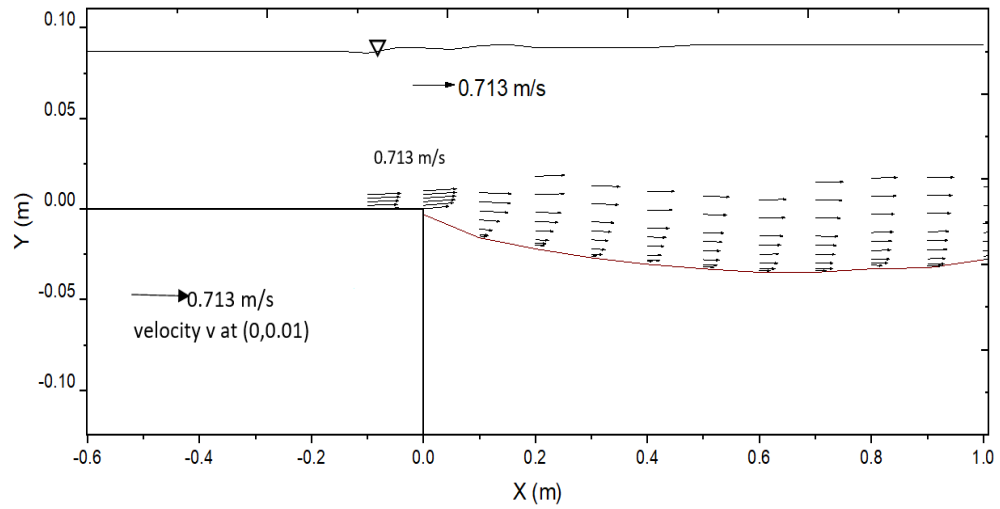


Fig 12 Velocity Vector plot of flow field inside maximum scour hole with smooth apron for Run 1A.

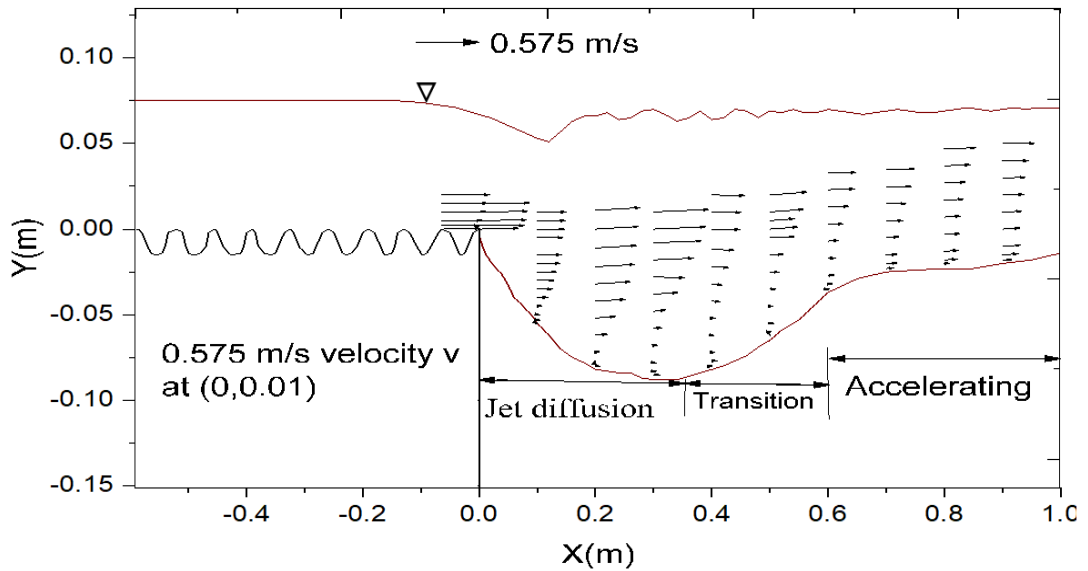
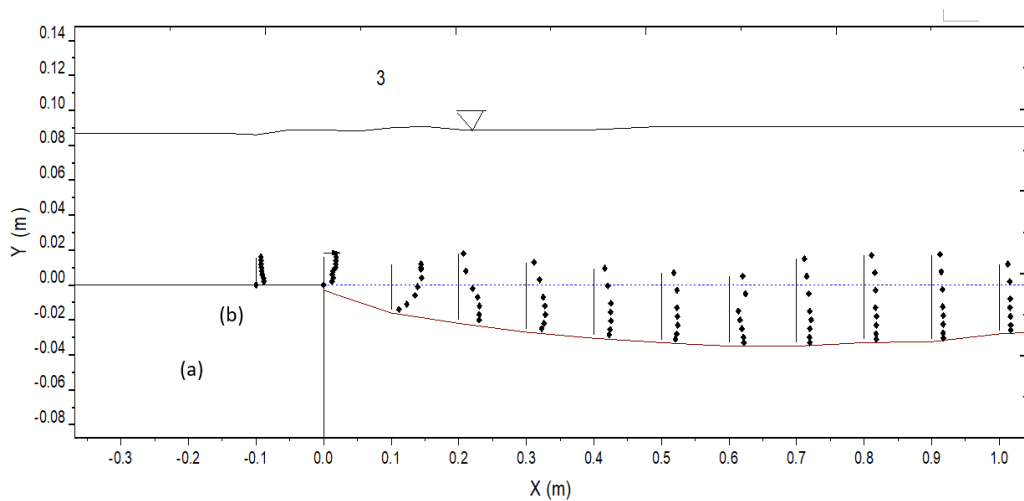


Fig 13 Velocity Vector plot of flow inside scour hole with corrugated apron for Run 9B



(a)

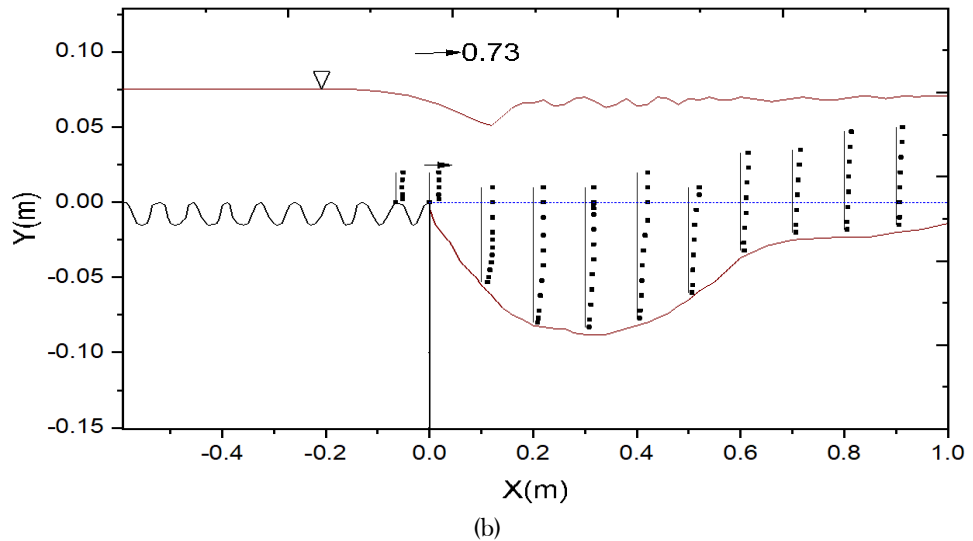


Fig 14 Vertical distribution of normalized turbulence intensity TI in scour hole for (a) Run 1A, and (b) Run 9B.

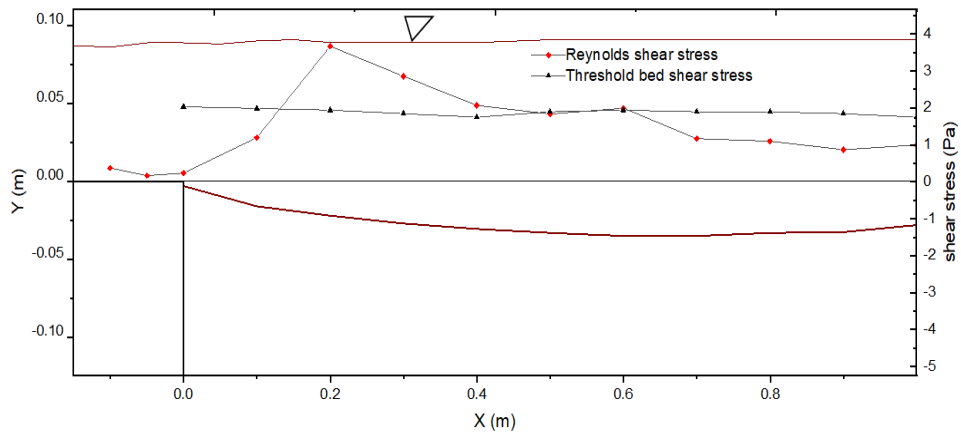


Fig 15 A comparison of threshold bed shear stress and Reynolds stress downstream of smooth apron Run 1A.

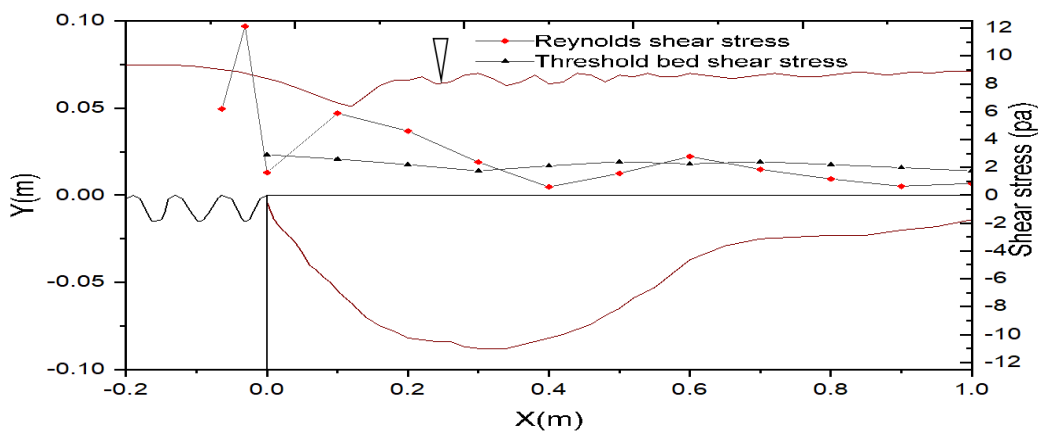


Fig 16 A comparison of threshold bed shear stress and Reynolds stress downstream of corrugated apron Run 9B

3.2.5 Bed shear stress

At equilibrium condition in clear water flow, forces acting on sediment particles in the scour hole are drag force exerted by fluid F_D , lift force F_L , and submerged weight W of particle. Considering those all forces, the critical shear stress in streamwise sloping bed is given by Chiew and Parker [21] as:

$$\frac{\tau'_c}{\tau_c} = \cos\theta' \left(1 + \frac{\tan\theta'}{\tan\phi} \right) \tag{4}$$

where τ'_c is the critical shear stress on sloping bed of angle θ' and τ_c = critical shear stress on horizontal bed computed using Shields diagram. Dimensionless critical shear stress is given as:

$$\frac{\tau_c}{(\gamma_s - \gamma_f)d} = 0.06 \text{ for coarser particles.}$$

Using this, $\tau_c = 1.748 \text{ Pa}$

The experimental bed shear stress is computed using Reynolds stress distribution [22]. Reynolds stress $\bar{\tau}_{x,y}$ is computed as $\overline{u'v'}$. For sloping bed,

$$[\bar{\tau}_{x,y}]_{\theta'} = \cos\theta' \rho u'v' \quad (5)$$

For every 0.1 m interval, θ' was computed. Threshold bed shear stress and Reynolds stress were computed using Equation (4) and (5), respectively, as shown in Figures 15 and 16. Figure 15 shows that threshold bed shear stress decreases with streamwise distance along x. The experimental bed shear stress computed from Reynolds stress distribution shows that initially it decreases on smooth apron as distance increases and as it leaves apron, there is some drastic increase of shear stress which is due to change in surface from smooth to rough. Further, its value goes on decreasing. Similarly, in case of corrugated apron, Reynolds stress developed on apron is about ten times higher than smooth apron. It decreases on edge of crest of apron and further increases due to change in surface. Further, it goes on decreasing as shown in Figure 16.

4. Conclusions

Experiments were performed in free flow condition for scour downstream of corrugated apron for different dimensions of corrugations having constant length of apron as well as uniform size of sediment. Conclusions drawn from the above analysis are summarized below:

- In free flow subcritical condition, application of corrugation over the rigid apron increases scour depth as compared to smooth apron. It is due to higher turbulence intensity over corrugated apron than smooth apron.
- Scour downstream of corrugated apron clearly shows three distinct regions: jet diffusion, transition and accelerating region as well as recirculating region at near bed of scour hole.
- Rate of increase of turbulence intensity in scour hole due to smooth apron was found to be higher than scour hole due to corrugated apron, although turbulence intensity in scour hole due to corrugated apron was higher than smooth apron.
- The Reynolds shear stress near corrugated apron surface is found to be nearly ten times higher than smooth rigid apron and it increases as it leaves apron to scour hole due to change in surface and decreases longitudinally towards downstream. There is a slight increase in Reynolds shear stress up to certain distance in downstream slope of scour hole, then it decreases linearly where flow starts to accelerate just after downstream slope of scour hole.
- Similarly, threshold bed shear stress follows the same trend as of Reynolds shear stress longitudinally towards downstream.
- In free flow condition, corrugated apron gives adverse result than smooth apron. Generally, we open sluice gate fully during maintenance period. Hence, care should be taken during that period.
- Turbulence intensity and shear stress governs the scour profile.

References

- [1] Chatterjee, S. S., and Ghosh, S. N. (1980). Submerged horizontal jet over erodible bed. *Journal of Hydraulics Division*, 106(11), 1765-1782.
- [2] Hassan, N. M. K. N., and Narayanan, R. (1985). Local Scour Downstream of an Apron. *Journal of Hydraulic Engineering*, 111(11), 1371-1385.
- [3] Ali, K. H. M., and Lim, S. Y. (1986). Local scour caused by submerged wall jets. *Proceedings of the Institution of Civil Engineers*, 81(2), 607-645.
- [4] Chatterjee, S. S., Ghosh, S. N., and Chatterjee, M. (1994). Local scour due to submerged horizontal jet. *Journal of Hydraulic Engineering*, 120(8), 973-992.
- [5] Aderibigbe, O., and Rajaratnam, N. (1998). Effect of sediment gradation on erosion by plane turbulent wall jets. *Journal of Hydraulic Engineering*, 124(10), 1034-1042.
- [6] Rajaratnam, N., and Ead, S.A. (2000). Turbulent Open Channel Flow in Circular Corrugated Culverts. *Journal of Hydraulic Engineering*, 126(October), 750-757.
- [7] Dey, S., and Sarkar, A. (2006). Scour Downstream of an Apron Due to Submerged Horizontal Jets. *Journal of Hydraulic Engineering*, 132(3), 246-257.
- [8] Sarkar, A., and Dey, S. (2008). Characteristics of Turbulent Flow in Submerged Jumps on Rough Beds. *Journal of Engineering Mechanics*, 134(7), 599-599.
- [9] Farhoudi, J., and Smith, K. V. H. (2010). Local scour profiles downstream of hydraulic jump. *Journal of Hydraulic Research*, 23(4), 343-358.
- [10] Guan, D., Melville, B. W., and Friedrich, H. (2014). Flow Patterns and Turbulence Structures in a Scour Hole Downstream of a Submerged Weir. *Journal of Hydraulic Engineering*, 140(1), 68-76.
- [11] Aamir, M., and Ahmad, Z. (2015). Estimation of scour depth downstream of an apron under 2D horizontal jets. *Proceedings of HYDRO 2015 International, 20th International Conference on Hydraulics, Water Resources and River Engineering, Indian Institute of Technology Roorkee, India*.
- [12] Aamir, M., and Ahmad, Z. (2017). Prediction of local scour depth downstream of an apron under wall jets. In: *Garg V., Singh V., Raj V. (eds) Development of Water Resources in India. Water Science and Technology Library, Springer, Cham*, 75(32), 375-385.
- [13] Aamir, M., and Ahmad, Z. (2019). Estimation of maximum scour depth downstream of an apron under submerged wall jets. *Journal of Hydroinformatics*, 21(4), 523-540.
- [14] Peterka, A.J. (1984). Hydraulic Design of Stilling Basins and Energy Dissipators. *Bureau of Reclamation* (25).
- [15] Helal, E. Y., Nassralla, T. H., and Abdelaziz, A. A. (2013). Minimizing of scour downstream hydraulic structures using sills. *International Journal of Civil and Structural Engineering*, 3(3).

- [16] Pillai, N. N., and Unny, T. E. (1964). Shapes for Appurtenances in Stilling Basins. *Journal of Hydraulic Division*, 90(3), 1-21.
- [17] Aamir, M., and Ahmad, Z. (2016). Review of literature on local scour under plane turbulent wall jets. *Physics of Fluids*, 28, 105102.
- [18] Rajaratnam, N., and Ead, S.A. (2002). Hydraulic Jumps on Corrugated Beds. *Journal of Hydraulic Engineering*, 128(7) July 1, 2002.
- [19] Ali, H. M., El Gendy, M. M., Mirdan, A. M. H., Ali, A. A. M., and Abdelhaleem, F. S. F. (2014). Minimizing downstream scour due to submerged hydraulic jump using corrugated aprons. *Ain Shams Engineering Journal*, 5(4), 1059-1069.
- [20] Basiouny, M. E., Nasrallah, T. H., Abdelhaleem, F. S., and Ibraheem, A. S. (2018). Roughened and Corrugated aprons as scour countermeasure downstream of submerged hydraulic jump, *Twenty-first International Water Technology Conference, IWTC21*, pp. 200-214.
- [21] Chiew, Y. M., and Parker, G. (1994). Incipient sediment motion on non-horizontal slopes: Début d'entraînement de sédiments sur des lits non horizontaux. *Journal of Hydraulic Research*, 32(5), 649-660.
- [22] Dey, S., Sarkar, S., and Solari, L. (2011). Near-Bed Turbulence Characteristics at the Entrainment Threshold of Sediment Beds. *Journal of Hydraulic Engineering*, 137(9), 945-958.

© 2019 by the authors. Submitted for possible open access publication under the terms and conditions of the Creative Commons Attribution (CC BY) license (<http://creativecommons.org/licenses/by/4.0/>).



Appendix

Table 1 Experimental data for free flow condition

Smooth rigid apron					
Runs	V (m/s)	F	Y _i (m)	Y _f (m)	d. (m)
1A	0.51	0.57	0.082	0.09	0.0484
2A	0.57	0.68	0.0725	0.08	0.074
3A	0.59	0.7	0.071	0.07	0.0825
4A	0.61	0.75	0.07	0.06	0.094
Corrugated apron					
Runs	V (m/s)	F	Y _i (m)	Y _f (m)	d. (m)
Corrugated apron, S=70 mm & t= 20 mm					
1B	0.51	0.57	0.082	0.09	0.142
2B	0.57	0.68	0.0725	0.08	0.152
3B	0.59	0.7	0.071	0.07	0.17
4B	0.61	0.75022	0.07	0.06	0.185
Corrugated apron, S=70 mm & t= 15 mm					
5B	0.51	0.57	0.082	0.09	0.0725
6B	0.57	0.68	0.0725	0.08	0.0958
7B	0.59	0.7	0.071	0.07	0.105
8B	0.6	0.72	0.07	0.06	0.11
Corrugated apron, S=65 mm & t= 15 mm					
9B	0.51	0.57	0.082	0.09	0.0825
10B	0.57	0.68	0.0725	0.08	0.108
11B	0.59	0.7	0.071	0.07	0.115
12B	0.6	0.72	0.07	0.06	0.117
Corrugated apron, S=70 mm & t= 25 mm					
13B	0.51	0.57	0.082	0.09	0.152
14B	0.57	0.68	0.0725	0.08	0.176
15B	0.59	0.7	0.071	0.07	0.19
16B	0.6	0.72	0.07	0.06	0.195